International Journal of Microwave and Wireless Technologies

cambridge.org/mrf

Bandwidth improvement of planar antennas using a single-layer metamaterial substrate for X-band application

O. Borazjani[1], M. Naser-Moghadasi[1], J. Rashed-Mohassel[2] and R. A. Sadeghzadeh[3]

[1]Department of Electrical and Computer Eng., Science and Research Branch, Islamic Azad University, Tehran, Iran; [2]School of ECE, College of Engineering, University of Tehran, Tehran, Iran and [3]Department of Electrical and Computer Eng., K. N. T. University of Technology, Tehran, Iran

Research Paper

Cite this article: Borazjani O, Naser-Moghadasi M, Rashed-Mohassel J, Sadeghzadeh RA (2020). Bandwidth improvement of planar antennas using a single-layer metamaterial substrate for X-band application. *International Journal of Microwave and Wireless Technologies* **12**, 906–914. https://doi.org/10.1017/S1759078720000264

Received: 26 September 2019
Revised: 3 March 2020
Accepted: 5 March 2020
First published online: 6 April 2020

Key words:
Bandwidth; electromagnetic band gap (EBG) structure; metamaterial; patch antenna; X-band

Author for correspondence:
J. Rashed-Mohassel,
E-mail: jrashed@ut.ac.ir

Abstract

To prevent far-field radiation characteristics degradation while increasing bandwidth, an attempt has been made to design and fabricate a microstrip antenna. An electromagnetic band gap (EBG) structure, including a layer of a metallic ring on a layer of Rogers 4003C substrate, is used. For a better design, a patch antenna with and without the EBG substrate has been simulated. The results show that the bandwidth can be improved up to 1.6 GHz in X-band by adding the EBG substrate. Furthermore, using this structure, a dual-band antenna was obtained as well. Finally, to validate the simulation results, a comparison has been done between simulation data and experimental results which demonstrate good agreement.

Introduction

Nowadays, antennas must be small, have a low profile, with high operating bandwidth and considerable directivity. Low profile patch antennas with simple structures and with the capability of fabricating on printed circuit boards (PCB) can be considered as suitable alternatives. However, two disadvantages of these antennas are narrow bandwidth and low directivity. To achieve wide bandwidth and yet a small size, patch antennas are made on thick high dielectric constant substrates [1]. A high dielectric constant leads to an increased cost of fabrication with the propagation of unwanted modes in the substrate, which affects the antenna's radiation characteristics [1, 2].

Another way to overcome these disadvantages is by using artificial metamaterials [3–9]. There are numerous classifications for metamaterial structures in the literature and electromagnetic band gaps (EBG) are categorized as one of these classifications [10, 11].

Applying EBG structures leads to many new antennas and applications [12–14]. These structures can remove the unwanted effects of substrates and cause gain enhancement [15–17].

They are used to control the propagation of electromagnetic waves. The application of EBG is based on wave propagation either as a filter or as a defect in a periodic structure. The latter is useful in antenna applications to radiate EM waves in the desired direction at a specified frequency. EBGs usually behave as band-stop filters [18, 19], rejecting the energy flow over a fixed band of frequencies and can be used in absorption applications [20, 21]. Also, they can be used in optical applications [22, 23]. When a defect is introduced affecting the periodicity of the structure; a region of localized electromagnetic energy is established. The patch antenna is considered as the defect of a structure.

In this paper, the design of an antenna for X-band with an increase of the bandwidth of a simple rectangular microstrip antenna is contemplated. In many previous works [24–26], substrates or superstrates have been used to enhance the bandwidth of microstrip antennas. In the present work, to fabricate a broadband microstrip antenna, a single-layer EBG substrate with a ring resonator structure is designed. To do this, the basic shape and dimensions are selected using experimental results and the available data in the literature. To achieve higher bandwidth, the antenna is simulated and optimal parameters such as dielectric thickness and structure dimensions are obtained using a parameter study. Finally, based on simulation results, a patch antenna is fabricated and experimental data are compared with the simulation results.

Design and simulation

EBG unit-cell design and simulation

In this section, the EBG substrate is designed. The equivalent circuit of conventional mushroom EBG structures is shown in Fig. 1. In this EBG structure, vias and the patches play the roles of parallel and series inductors, respectively. The gap between the two elements of

© Cambridge University Press and the European Microwave Association 2020

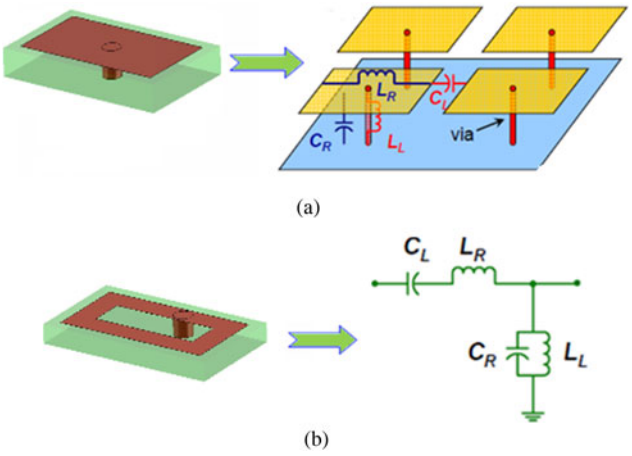


Fig. 1. The equivalent circuit of the EBG unit cell: (a) conventional unit cell, (b) ring resonator unit cell.

the single cell constitutes the series capacitor, while the ground plane and the patch are modeled as a parallel capacitor.

The equivalent circuit [27] of the structure used in this article is the same except the EBG structure can better control the inductances [28, 29].

The bandwidth of the planar antenna associated with the inductance and capacitance of the equivalent circuit is [30]

$$BW \propto \sqrt{\frac{L}{C}}, \tag{1}$$

where inductances are given by [8, 31, 32]

$$\begin{aligned} L_R &= \frac{\mu_0}{\pi}\sqrt{e^2+f^2}\left[\sqrt{2}\,Ln\frac{2\sqrt{e^2+f^2}}{w}-1\right] \\ L_{via} &= 5\cdot 08\,t\left(Ln\frac{2t}{r}-1\right). \end{aligned} \tag{2}$$

In which "e" and "f" are ring dimensions and "w" is the width of its strip as shown in Fig. 2. Therefore,

$$BW \propto \sqrt{\frac{\mu_r}{\varepsilon_r}}. \tag{3}$$

According to equation (2), in addition to the unit-cell dimensions, the ring width, w, is also one of the parameters affecting the inductive property and consequently the resonant frequency of the structure.

To calculate the relative permeability, relative permittivity, and the refractive index of the EBG unit cell, the ring resonator unit cell with boundary conditions given in Fig. 3 is simulated in CST. PEC boundary conditions are used on two sides and PMC was used on the other two, indicating the periodic structure. To excite the structure, two wave ports were used and the relative permeability, the relative permittivity, and the refractive index were extracted from the S parameters [33].

$$S_{11} = S_{22} = -\frac{1}{2}\left(z-\frac{1}{2}\right)\sin(nkh), \tag{4}$$

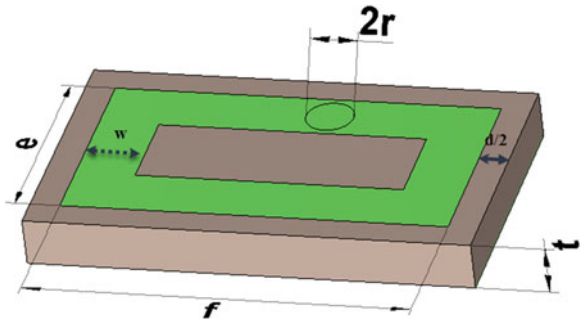


Fig. 2. Ring resonator unit cell.

$$S_{12} = S_{21} = \frac{1}{\cos(nkh) - \frac{i}{2}(z+\frac{1}{z})\sin(nkh)}. \tag{5}$$

Equations (4) and (5) result in:

$$z = \sqrt{\frac{(1+S_{11})^2 - S_{21}^2}{(1-S_{11})^2 - S_{21}^2}}, \tag{6}$$

$$n = \frac{1}{kh}\cos^{-1}\left[\frac{1}{2S_{21}}(1-S_{11}^2+S_{21}^2)\right], \tag{7}$$

$$\varepsilon = \frac{n}{z},\ \mu = nz. \tag{8}$$

With an increased relative permeability and a decreased relative permittivity of a material, wider operation bandwidth can be achieved. The EBG structure can increase the inductance of the circuit and therefore results in bandwidth improvement. Relative permeability of the ring resonator unit cell and a conventional unit cell of the same area are shown in Fig. 4. As can be observed, the relative permeability of the ring resonator unit cell can be changed simply by varying its width, w. This can be ascribed to yet another degree of freedom which leads to increased inductive properties and, as a result, an improved bandwidth.

A parametric study is performed to select the dimensions of the unit cell for a resonant frequency of 9.7 GHz. The parameter "d" is the periodicity of the neighboring cells. The results are illustrated in Tables 1–5. As can be seen, the parameters "e", "f", and "d" do not significantly change the resonant frequency while "t" and "w" affect the resonant frequency of the structure. The final values of these parameters for the resonant frequency of 9.7 GHz are shown in Table 6. The constitutive parameters of the optimized EBG unit cell are illustrated in Table 7.

EBG substrate design and simulation

To obtain an improved bandwidth for a transmission coefficient, S_{21}, lower than −10 dB, the rings and vias dimensions and vias locations are the parameters to be optimized. The EBG structure used in this paper (Fig. 5) includes a 4 × 9 array of square rings on a layer of Rogers 4003C ($\varepsilon_r = 3.58$) with 0.8 (mm) thickness and a

https://doi.org/10.1017/S1759078720000264 Published online by Cambridge University Press

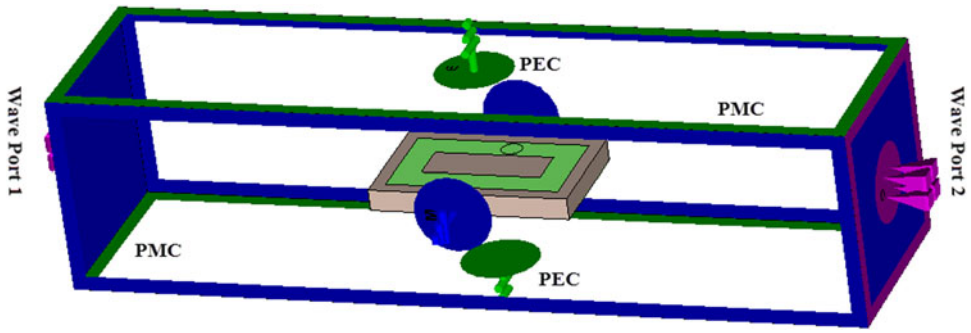


Fig. 3. Boundary conditions of the simulated ring resonator of the EBG unit cell.

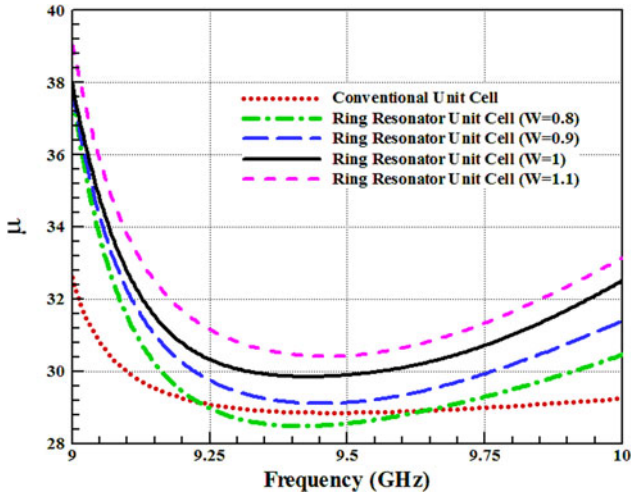


Fig. 4. Relative permeability of the conventional mushroom unit cell and the ring resonator unit cell for different widths of the ring, *w* (mm).

Table 1. Effect of parameter "*e*" on the resonant frequency

"*e*" (mm)	Fr (GHz)
3	9.76
3.5	9.69
4	9.63

Table 2. Effect of parameter "*f*" on the resonant frequency

"*f*" (mm)	Fr (GHz)
6	9.76
6.5	9.69
7	9.63

Table 3. Effect of parameter "*t*" on the resonant frequency

"*t*" (mm)	Fr(GHz)
0.8	9.67
1.2	9.5
1.6	9.34
2	9.14

Table 4. Effect of parameter "*d*" on the resonant frequency

"*d*" (mm)	Fr (GHz)
0.6	9.66
0.8	9.68
1	9.67
1.2	9.65
1.4	9.63

Table 5. Effect of parameter "*w*" on the resonant frequency

"*w*" (mm)	Fr (GHz)
0.5	9.79
0.6	9.77
0.7	9.76
0.8	9.73
0.9	9.72
1	9.68
1.1	9.64
1.2	9.62
1.3	9.52
1.4	9.44
1.5	9.36

Table 6. Dimensions of the unit cell

e (mm)	*f* (mm)	*t* (mm)	*d* (mm)	*r* (mm)	*w* (mm)
3.5	6.5	0.8	0.8	0.5	1

Table 7. Constitutive parameters of the EBG unit cell

f_{res}	value of ε	value of μ	value of *n*
9.7	0.8	30.38	0

ground plane of 40 mm × 30 mm. The square patch antenna is designed to operate at 9.7 GHz.

To find the stopband of the EBG substrate, the two ports are assumed at the opposite edges of the bottom and a transmission

https://doi.org/10.1017/S1759078720000264 Published online by Cambridge University Press

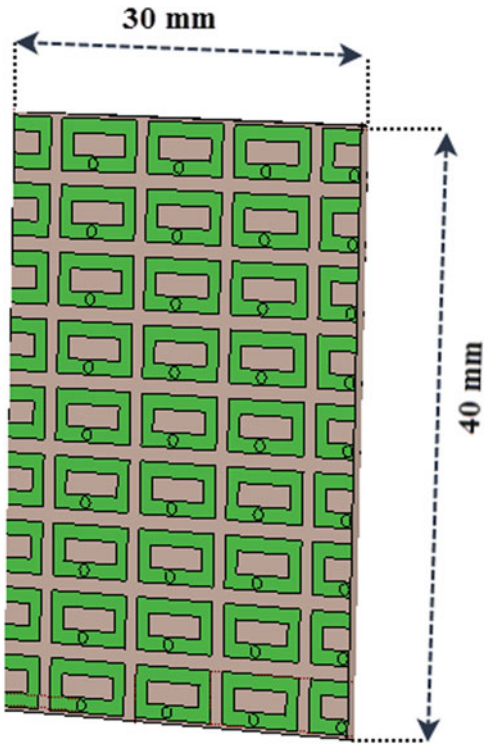


Fig. 5. The schematic configuration of the electromagnetic band gap (EBG) layer.

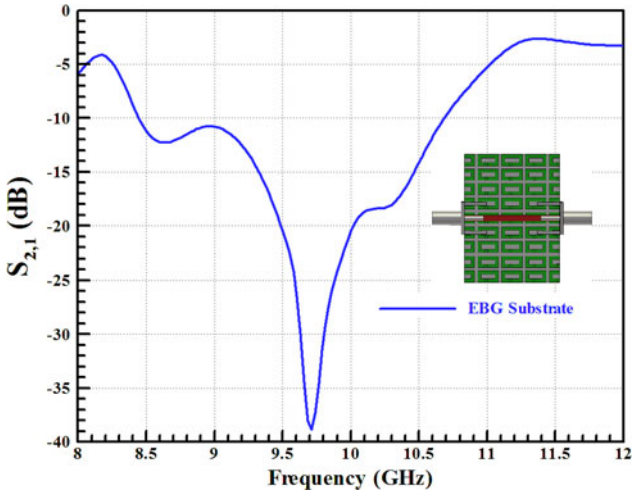


Fig. 6. S_{21} versus frequency for the EBG and the schematic representation of the transmission line on the EBG structure.

line is located on the top of the EBG structure. The scattering parameters can then be extracted as shown in Fig. 6. The transmission coefficient, S_{21}, is calculated by exiting the ports. The stopband, defined for S_{21} lower than −10 dB, is obtained as 8.4–10.7 GHz and the resonant frequency is 9.7 GHz as expected.

Patch antenna simulation

A conventional patch antenna is designed at 9.7 GHz. To excite the antenna, a microstrip line with a width of 1.9 mm is used corresponding to an input impedance of 50 Ω. Two gaps with the

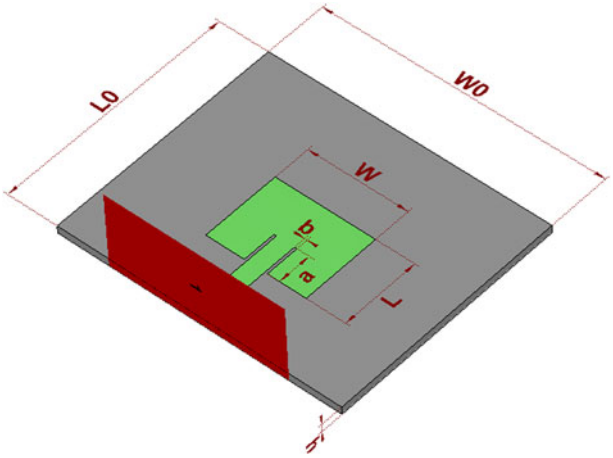


Fig. 7. The schematic representation of the conventional antenna.

Table 8. Dimensions of the antenna

Specifications	Dimensions (mm)
Patch width, W	10.3
Patch length, L	7.9
Gap width, a	3.5
Gap length, b	0.26
Substrate width, W_0	40
Substrate length, L_0	30
Substrate thickness, h	0.8

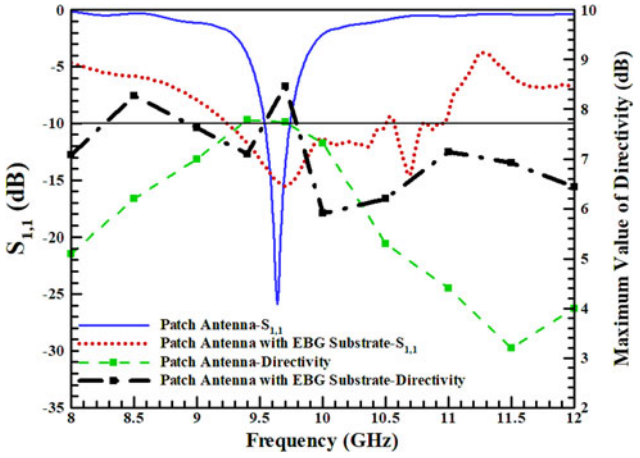


Fig. 8. Reflection coefficient and maximum directivity of the patch antenna with and without the EBG substrate.

dimensions of 3.5 (mm) × 0.26 (mm) are used for proper impedance matching as shown in Fig. 7. The 10 dB return loss bandwidth is 0.2 GHz and the gain at resonance is 7.71 dBi. The dimensions of the patch antenna are obtained by antenna design equations [34]. For impedance matching, the inset feed is used as shown in Fig. 7.

The dimensions of the designed antenna at 9.7 GHz are given in Table 8.

https://doi.org/10.1017/S1759078720000264 Published online by Cambridge University Press

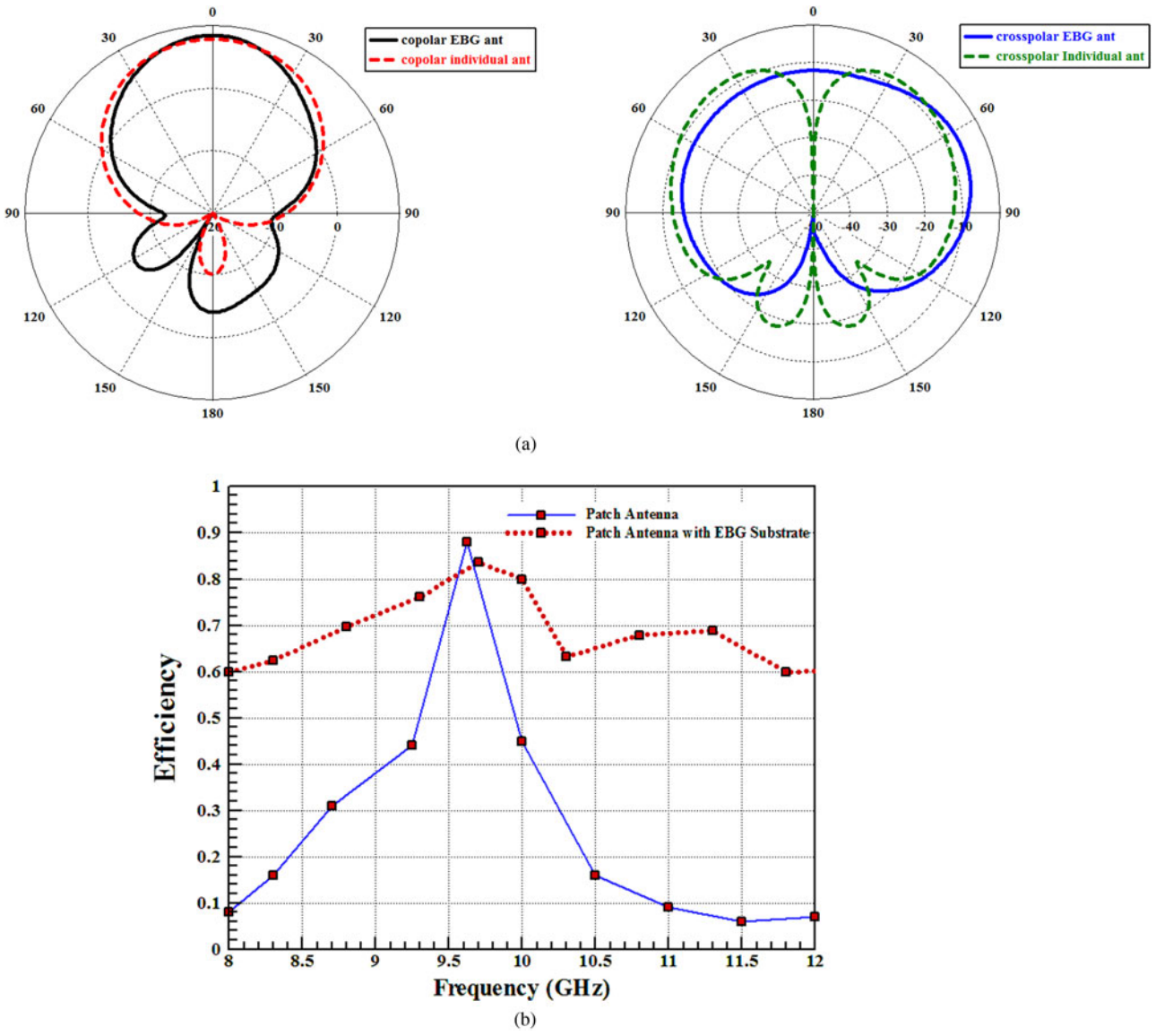


Fig. 9. (a) Radiation pattern of the patch antenna with and without the EBG substrate at 9.7 (GHz). (b) The efficiency of the patch antenna with and without the EBG substrate.

Results and discussion

An EBG ring resonator was designed and simulated in this work. This EBG structure has the potential to better control the inductive properties and therefore increase the bandwidth. The bandwidth of a microchip patch antenna in the X-band is then increased by only one substrate. To achieve this, an array of 4 × 9 was designed and simulated.

The simulated reflection coefficient, S_{11}, and maximum directivity of the conventional patch antenna with and without the EBG substrate are illustrated in Fig. 8. As can be observed, the antenna bandwidth with the EBG substrate is 1.8 GHz which is increased to about 1.6 GHz, and the maximum directivity fluctuations of the metamaterial antenna are less than the conventional antenna in the desired bandwidth. As it is observed in Fig. 8, it can be concluded that the EBG substrate antenna can operate well in all frequencies of the bandwidth compared with the conventional patch antenna. Therefore, with the EBG substrate, a wideband antenna is achieved which is useful in broadband applications. Furthermore, maximum directivity for the patch antenna with EBG substrate is 8.43 dBi and the 3 dB bandwidth covers the entire X-band frequencies which are prominent in industrial and military applications.

The radiation characteristics of the proposed antenna are also discussed. The corresponding radiation pattern for the antenna with the EBG substrate at 9.7 GHz is illustrated in Fig. 9(a). The polarization of the individual antenna is linear and has not been changed when the EBG structure is used as the substrate. Figure 9(a) shows that the directivity of the metamaterial antenna is increased by 0.72 dB and the back lobe level is higher than the conventional antenna. The cross-polar radiation pattern of the metamaterial antenna is increased at some angles in comparison to a normal antenna while it is decreased in some other directions.

Figure 9(b) shows that the radiation efficiency of the EBG antenna is significantly higher than typical antenna efficiency

https://doi.org/10.1017/S1759078720000264 Published online by Cambridge University Press

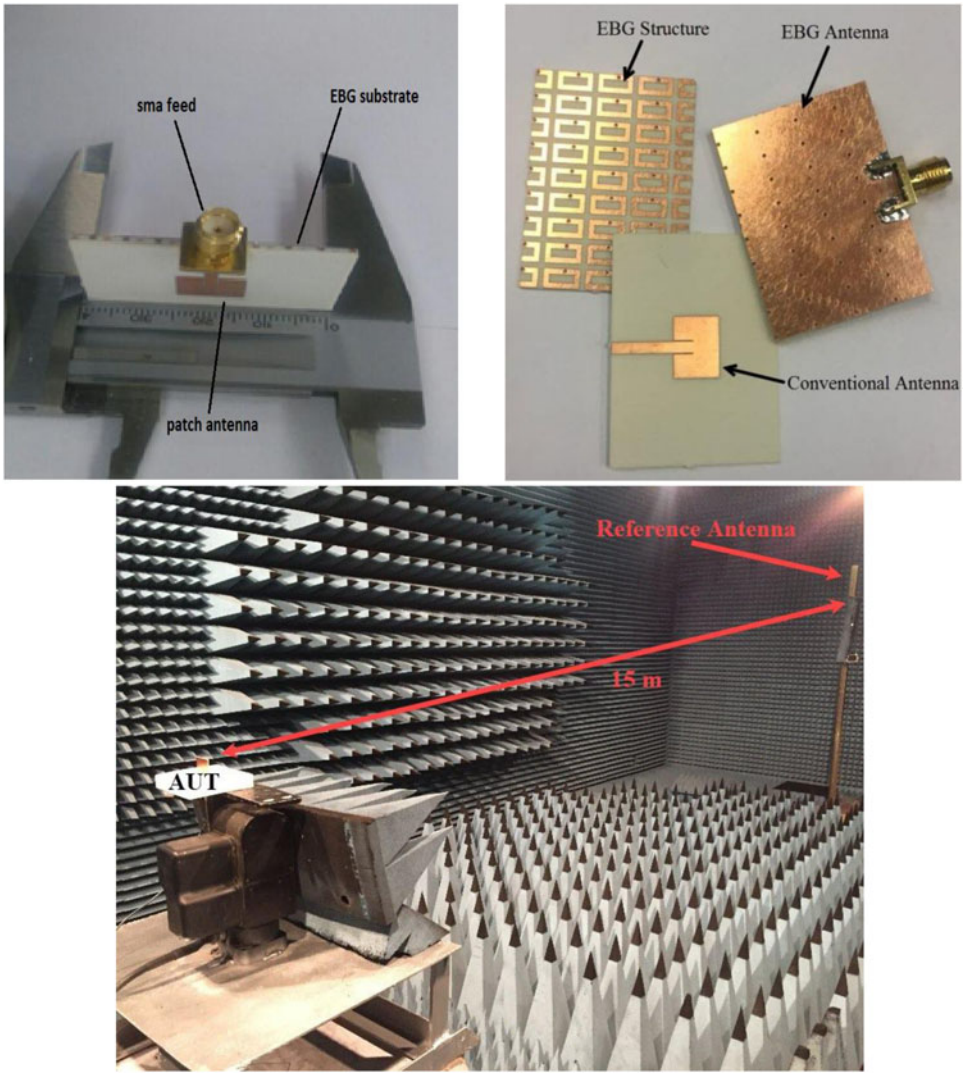


Fig. 10. Construction and experimental setup.

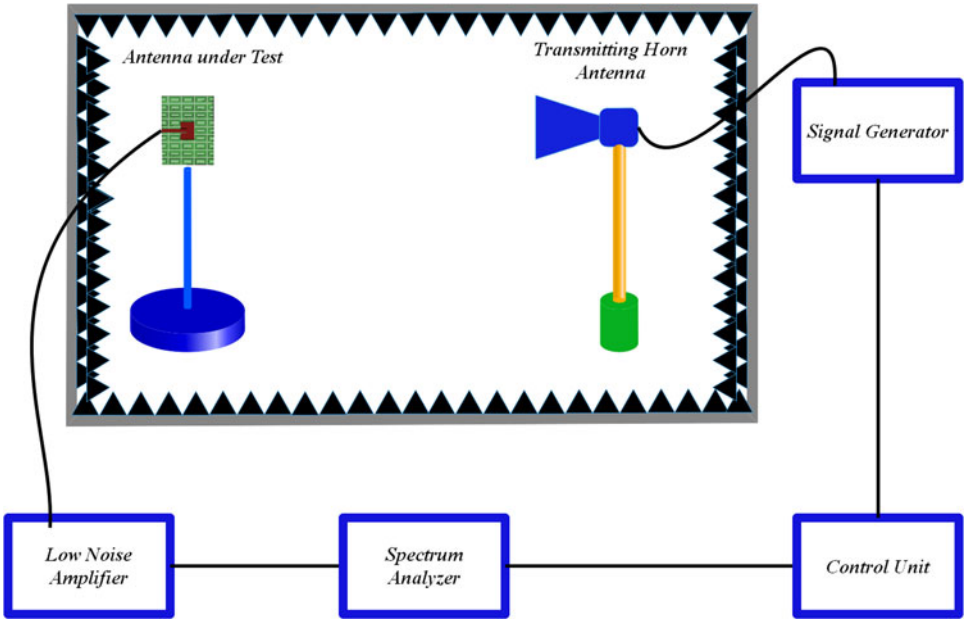


Fig. 11. Schematic representation of the experimental setup.

https://doi.org/10.1017/S1759078720000264 Published online by Cambridge University Press

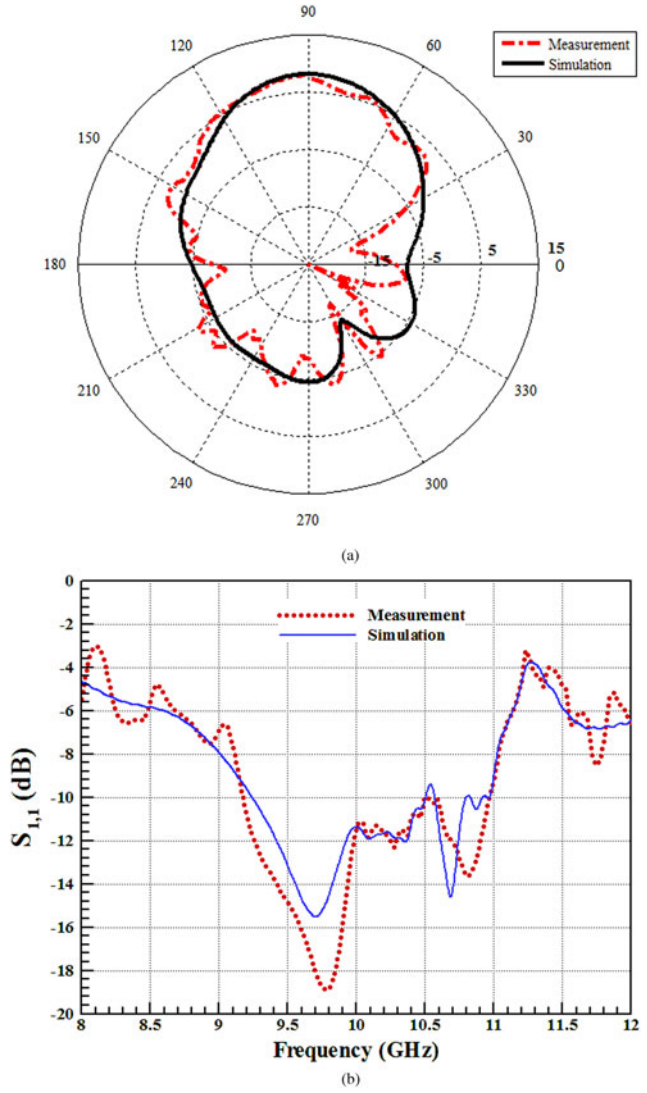


Fig. 12. (a) The simulated and measured radiation pattern of EBG antenna, (b) The simulated and measured S_{11} of EBG antenna.

over the entire bandwidth. The radiation efficiency is well above 0.6 (60%) for the X-band frequency range and yet with favorable directivity for all frequencies in the bandwidth. Therefore, it can be used in broadband antenna applications.

The desired antenna was fabricated and the experiments were performed in an anechoic chamber as shown in Fig. 10. The schematic representation of the experimental set up is shown in Fig. 11. To obtain the radiation pattern, the antenna was placed in a chamber with a length of 15 m, where the separation of the transmitting antenna and the antenna under test exceeds the far-field distance criteria. The structure of the patch antenna with the EBG substrate has been examined using simulation as well as measured data. Figure 12 shows the measured and simulated radiation patterns and S_{11} of the patch antenna with the metamaterial substrate. The return loss bandwidth below −10 dB of the EBG antenna is around 1.8 GHz. The measured return loss of EBG antennas reveals a slight shift in the resonances toward higher frequencies than those designated by simulation. This shift is attributed to fabrication inaccuracies and the connector assembly. The simulation and measured results are in good agreement.

Table 9 presents a comparison of bandwidths and gain improvement, sizes, and previously reported works. It is concluded that the present work improves the bandwidth for approximately 1.6 GHz and the directivity for about 0.72 dB. Also, compared with previous works in the X-band [8, 35–38], the structure is smaller in size and more simple with fewer numbers of layers. As for the effects of metamaterial substrate on radiation pattern, previous works show some squint and deviation. In the present paper, although the gain of EBG structure does not show a drastic increase, it does not affect the shape of the radiation pattern, which is crucial in data transmission, industrial, and military applications.

Conclusion

A microstrip antenna with an EBG structure as a substrate was designed and fabricated in the X-band. Experimental results were compared with simulation data and good agreement was observed. Using the ring resonant structure in the EBG substrate increases the inductances of the structure in comparison with conventional mushroom EBG structures which is a key parameter in the design. This structure has better control of resonant frequency and its larger inductances result in a smaller size for a given resonant frequency. Therefore, it can be used when miniaturization application is contemplated. CST software and parametric study were used to obtain optimal dimensions of the design. A ring-shaped metallic is used for the unit cell of the EBG structure. The bandwidth of a simple rectangular microstrip antenna was increased by as much as 1.6 GHz. Furthermore, the result is a dual-band structure; with two resonances at 9.8 and 10.8 GHz, and the return loss in these frequencies is less than −20 and −14 dB, respectively. The antenna directivity improvement is 0.72 dB. The polarization of the antenna with EBG is not changed compared to an individual antenna. A single EBG layer is used in the structure, which does not significantly affect the height of the antenna despite the use of an artificial ground

Table 9. Comparison of the performance of the presented EBG antennas in previous reports and this work

Reference	Frequency band	Size of antenna (width × length × thickness)	Complexity in fabrication	Bandwidth improvement(GHz)
This work	X-band	$1.25\lambda \times 0.9\lambda \times 0.04\lambda$	Simple	1.6
[8]	X-band	$1.43\lambda \times 1\lambda \times 0.04\lambda$	Complex	0.98
[35]	X-band	$0.16\lambda \times 0.19\lambda \times 0.1\lambda$	Complex	0.512
[36]	X-band	$1.14\lambda \times 1.14\lambda \times 0.97\lambda$	Complex	0.35
[37]	X-band	$1.4\lambda \times 1.87\lambda \times 0.04\lambda$	Complex	None
[38]	X-band	$2.4\lambda \times 2.4 \times 1.2\lambda$	Complex	1.6

https://doi.org/10.1017/S1759078720000264 Published online by Cambridge University Press

structure. Furthermore, this simple EBG antenna, while having favorable bandwidth and directivity, is easy to fabricate and has low cost in PCB processing, which makes it suitable for military and industrial applications.

References

1. **Schaubert DH, Pozar DM and Adrian A** (1989) Effect of microstrip antenna substrate thickness and permittivity: comparison of theories with experiment. *IEEE Transactions on Antennas and Propagation* **37**, 677–682.
2. **Horák J and Raida Z** (2009) Influence of EBG structures on the far-field pattern of patch antennas. *Radioengineering* **18**, 223–229.
3. **Palandöken M** (2011) *Artificial Materials Based Microstrip Antenna Design*. Rijeka, Croatia: InTech.
4. **Arora C, Pattnaik SS and Baral RN** (2017) Performance enhancement of patch antenna array for 5.8 GHz Wi-MAX applications using metamaterial inspired technique. *AEU – International Journal of Electronics and Communications* **79**, 124–131.
5. **Chandrasekaran KT, Karim MF, Nasimuddin and Alphones A** (2017) CRLH structure-based high-impedance surface for performance enhancement of planar antennas. *IET Microwaves, Antennas & Propagation* **11**, 818–826.
6. **Navarro-Tapia M, Esteban J and Camacho-Peñalosa C** (2013) Broadband slot array antenna with full-space steerable pattern in a composite right/left-handed waveguide. *Radio Science* **48**, 406–415.
7. **Garg P and Jain P** (2019) Design and analysis of a metamaterial inspired dual band antenna for WLAN application. *International Journal of Microwave and Wireless Technologies* **11**, 351–358.
8. **Patel SK, Argyropoulos C and Kosta YP** (2017) Broadband compact microstrip patch antenna design loaded by multiple split ring resonator superstrate and substrate. *Waves in Random and Complex Media* **27**, 92–102.
9. **Patel SK and Kosta Y** (2013) Triband microstrip-based radiating structure design using split ring resonator and complementary split ring resonator. *Microwave and Optical Technology Letters* **55**, 2219–2222.
10. **Rahmat-Samii Y and Mosallaei H** (2001) Electromagnetic band-gap structures: classification, characterization, and applications, 11th International Conference on Antennas and Propagation (ICAP 2001), Manchester, UK.
11. **Liu Y and Alexopoulos NG** (2007) Semianalytical formulation on the scattering of proximity equilibration cell closed ring photonic band gap structures. *Radio Science* **42**, 1–16.
12. **Kumar A, Kumar D, Mohan J and Gupta HO** (2014) Investigation of grid metamaterial and EBG structures and its application to patch antenna. *International Journal of Microwave and Wireless Technologies* **7**, 705–712.
13. **Abdalla MA, Al-Mohamadi AA and Mohamed IS** (2019) A miniaturized dual band EBG unit cell for UWB antennas with high selective notching. *International Journal of Microwave and Wireless Technologies* **11**(2019), 1035–1043.
14. **Verma A, Singh AK, Srivastava N, Patil S and Kanaujia BK** (2019) Slot loaded EBG-based metasurface for performance improvement of circularly polarized antenna for WiMAX applications. *International Journal of Microwave and Wireless Technologies* **12**(2020), 212–220.
15. **Kavousi H, Rashed-Mohassel J and Edalatipour M** (2017) Miniaturized patch antenna using a circular spiral-based metamaterial. *Microwave and Optical Technology Letters* **59**, 2276–2279.
16. **Kawdungta S, Jaibanauem P, Pongga R and Phongcharoenpanich C** (2017) Superstrate-integrated switchable beam rectangular microstrip antenna for gain enhancement. *Radioengineering* **26**, 431.
17. **Bakhtiari A, Sadeghzadeh RA and Moghadasi MN** (2018) Gain enhanced miniaturized microstrip patch antenna using metamaterial superstrates. *IETE Journal of Research* **65**(2019), 635–640.
18. **Gao MJ, Wu LS and Mao J** (2012) Notched ultra-wideband (UWB) bandpass filter with wide upper stopband based on electromagnetic bandgap (EBG) structures, 2012 International Conference on Microwave and Millimeter Wave Technology (ICMMT), Shenzhen, China.
19. **Palandoken M** (2012) *Metamaterial-Based Compact Filter Design, in Metamaterial*. Rijeka, Croatia: InTech.
20. **Deng T, Li ZW and Chen ZN** (2017) Ultrathin broadband absorber using frequency-selective surface and frequency-dispersive magnetic materials. *IEEE Transactions on Antennas and Propagation* **65**, 5886–5894.
21. **Ren J, Gong S and Jiang W** (2018) Low-RCS monopolar patch antenna based on a dual-ring metamaterial absorber. *IEEE Antennas and Wireless Propagation Letters* **17**, 102–105.
22. **Patel SK, Ladumor M, Parmar J and Guo T** (2019) Graphene-based tunable reflector superstructure grating. *Applied Physics A* **125**, 574–584.
23. **Patel SK, Ladumor M and Katrodiya D** (2019) Highly directive optical radiating structure with circular and diamond shape Si perturbations. *Materials Research Express* **6**, 1–16.
24. **Li M and Behdad N** (2012) Ultra-wideband, true-time-delay, metamaterial-based microwave lenses, the 2012 IEEE International Symposium on Antennas and Propagation, Chicago, IL, USA.
25. **Hadi RJ, Sandhagen C and Bangert A** (2014) Wideband high-gain multilayer patch antenna-coupler with metamaterial superstrate for x-band applications, 2014 44th European Microwave Conference, Rome, Italy.
26. **Mishra BP, Sahu S, Parashar SKS and Pathak SK** (2018) A compact wideband and high gain GRIN metamaterial lens antenna system suitable for C, X, Ku band application. *Optik* **165**, 266–274.
27. **Gangwar A and Gupta SC** (2014) Design of a single negative metamaterial based microstrip patch antenna. *International Journal of Computers and Applications* **98**, 4–8.
28. **Chen H, Ran L, Huangfu J, Grzegorczyk TM and Kong JA** (2006) Equivalent circuit model for left-handed metamaterials. *Journal of Applied Physics* **100**, 024915.
29. **Islam SS, Faruque MRI and Islam MT** (2014) The design and analysis of a novel split-H-shaped metamaterial for multi-band microwave applications. *Materials* **7**, 4994–5011.
30. **Yousefi L, Mohajer-Iravani B and Ramahi OM** (2007) Enhanced bandwidth artificial magnetic ground plane for low-profile antennas. *IEEE Antennas and Wireless Propagation Letters* **6**, 289–292.
31. **Jafargholi A and Mazaheri MH** (2015) Broadband microstrip antenna using epsilon near zero metamaterials. *IET Microwaves, Antennas & Propagation* **9**, 1612–1617.
32. **Paul CR** (2011) *Inductance: Loop and Partial*. New Jersey: John Wiley & Sons.
33. **Chen X, Grzegorczyk TM, Wu B-I, Pacheco J and Kong JA** (2004) Robust method to retrieve the constitutive effective parameters of metamaterials. *Physical Review E* **70**, 016608.
34. **Bhalla D and Bansal K** (2013) Design of a rectangular microstrip patch antenna using inset feed technique. *IOSR Journal of Electronics and Communication Engineering* **7**, 8–13.
35. **Joshi JG, Pattnaik SS, Devi S and Lohokare MR** (2010) Electrically small patch antenna loaded with metamaterial. *IETE Journal of Research* **56**, 373–379.
36. **Mali A, Hadi RJ, Khan MM, Sandhagen C and Bangert A** (2013) Enhancement of X band planar antenna parameters with zero index metamaterial, 2013 International Workshop on Antenna Technology (iWAT).
37. **Errifi H, Baghdad A, Badri A and Sahel A** (2014) Improving microstrip patch antenna directivity using EBG Superstrate. *American Journal of Engineering Research (AJER)* **3**, 125–130.
38. **Rahim T and Xu J** (2016) Design of high gain and wide band EBG resonator antenna with dual layers of same dielectric superstrate at X-bands. *Journal of Microwaves, Optoelectronics and Electromagnetic Applications* **15**, 93–104.



Omid Borazjani received his B.S and M.S degree in Electrical Telecommunication from the Islamic Azad University of Bushehr in 2006 and 2009. Now he is a Ph.D. student of Science & Research Branch, Islamic Azad University, Tehran. He has been a senior researcher and lecturer at the Islamic Azad University of Bushehr from 2009. His research interests are microstrip antenna design, microwave passive and active circuits, RF MEMS. E-mail: omidborazjani62@gmail.com

https://doi.org/10.1017/S1759078720000264 Published online by Cambridge University Press



Mohammad Naser-Moghadasi was born in Saveh, Iran, in 1959. He received the B.Sc. degree in Communication Engineering in 1985 from Leeds Metropolitan University (formerly Leeds Polytechnic), UK. Between 1985 and 1987, he worked as an RF design engineer for the Gigatech Company in Newcastle Upon Tyne, UK. From 1987 to 1989, he was awarded a full scholarship by the Leeds Educational Authority to pursue an M. Phil. degree studying in CAD of Microwave circuits. He received his Ph.D. degree in 1993, from the University of Bradford, UK. He joined Islamic Azad University, at Science & Research Branch, Iran, where currently he is an Associate Professor and Head of the Telecommunications group. His main areas of interest in research are microstrip antenna, microwave passive and active circuits, RF MEMS. He has so far published over 160 papers in different journals and conferences. E-mail: mn.moghaddasi@srbiau.ac.ir



Jalil Rashed-Mohassel was born in Birjand, Iran and received his Ph.D. degree in Electrical Engineering from the University of Michigan, Ann Arbor in 1982. His research interests include antennas, EM theory, and EMC/EMI. In 1994, he joined the University of Tehran where he is doing teaching and research as a professor in the school of ECE. He is the author of three books and has published more than 200 papers in refereed journals and conference proceedings. He is a principal member of the Center of Excellence on Applied Electromagnetic Systems (CEAES) and the director of the microwave laboratory. He is a distinguished professor and the recipient of several university and national prizes. Corresponding author. E-mail: jrashed@ut.ac.ir



Ramazanali Sadeghzadeh received the B.Sc. degree in Telecommunication Engineering from K. N. Toosi University of Technology, Tehran, Iran, in 1984; the M.Sc. degree in Digital Communication Engineering from the University of Bradford, Bradford, UK, and the University of Manchester Institute of Science and Technology (UMIST), Manchester, UK, as a joint program in 1987; and the Ph.D. degree in Electromagnetic and Antenna from the University of Bradford in 1991. During 1992–1997, he worked as a Postdoctoral Research Assistant in the field of propagation, electromagnetic, antenna, and wireless communication at the University of Bradford. From 1984 to 1985, he was with Iran Telecommunication Company, Tehran, Iran, working on networking. Since 1997, he has been with the Faculty of Electrical and Computer Engineering, K. N. Toosi University of Technology. He has published more than 200 referable papers in international journals and conferences. E-mail: sadeghz@eetd.kntu.ac.ir

https://doi.org/10.1017/S1759078720000264 Published online by Cambridge University Press